Meteorol Atmos Phys 92, 45–66 (2006)
DOI 10.1007/s00703-005-0112-4

Meteorology and Atmospheric Physics
Printed in Austria

Institut für Meteorologie und Klimaforschung, Universität Karlsruhe/Forschungszentrum Karlsruhe, Karlsruhe, Germany

A two-moment cloud microphysics parameterization for mixed-phase clouds. Part 1: Model description

A. Seifert and **K. D. Beheng**

With 2 Figures

Received October 15, 2003; revised July 9, 2004; accepted December 21, 2004
Published online: October 18, 2005

Summary

A two-moment microphysical parameterization for mixed-phase clouds was developed to improve the explicit representation of clouds and precipitation in mesoscale atmospheric models. The scheme predicts the evolution of mass as well as number densities of the five hydrometeor types cloud droplets, raindrops, cloud ice, snow and graupel. Since the number concentrations of all these hydrometeors are calculated explicitly, all relevant homogenous and heterogenous nucleation processes have been parameterized including the activation of cloud condensation nuclei, which is not predicted in most state-of-the-art cloud resolving models. Therefore the new scheme can discriminate between continental and maritime conditions and can be used for investigations of aerosol effects on the precipitation formation in mixed-phase clouds. In addition, the scheme includes turbulence effects on droplet coalescence, collisional breakup of raindrops and size-dependent collision efficiencies. A new general approximation of the collection kernels and the corresponding collision integrals is introduced.

1. Introduction

Clouds are an important part of the atmosphere and the climate system, since they determine and influence a variety of atmospheric processes/states. The representation of clouds in atmospheric models has to be paid particular attention, as the formation and spatial distribution of clouds and precipitation is crucial for numerical weather prediction (NWP) as well as for climate modeling.

Unfortunately, each individual cloud itself is a very complex non linear sub-system of the atmosphere and the delicate problem with cloud and precipitation modeling is to find a compromise between a very detailed but costly description in terms of spectral balance equations for the size distributions of many types of hydrometeors (cf. Khain et al, 2000, for a review) and a coarse but efficient parameterization in terms of equations dealing with certain integrals of the size distributions (e.g., only mass densities).

The latter approach is commonly used in forecast models and has shown a certain ability to describe large scale precipitation systems, but regional climate modeling and mesoscale NWP demand a more accurate approach. This is all the more important as recent observations indicate a strong anthropogenic influence on convective clouds and precipitation by aerosol modification (Rosenfeld, 2000). Unfortunately, the spectral cloud models are still too expensive to be useful for full 3-D simulations, while the common parameterized models are not able to represent aerosol-cloud interactions at all.

The importance of finding an efficient, i.e. parameterized, representation of the cloud microphysics was recognized very early in cloud modeling history. One of the first essential parameterization approaches is the famous scheme of Kessler (1969), who simplified the description of clouds and their processes by taking into account only mass densities where he originally concentrated on ''warm clouds''. The so-called Kessler scheme is based on two basic ideas: first, to distinguish formally between cloud droplets and raindrops and, second, to formulate the cloud processes relevant to this distinction in terms of time rates of change of mass densities. Partly by intuition and partly by applying simplistic considerations Kessler arrived at equations which have a long-standing tradition in cloud microphysics modeling. Within his approach Kessler introduced the terms ''autoconversion'' and ''accretion'' as those mechanisms converting cloud droplets to raindrops and growth of raindrops by collecting cloud droplets, respectively. A drawback of Kessler's formulae is that they do not take into account any characteristic of an underlying cloud droplet spectrum, i.e. they are not able to distinguish between maritime and continental clouds, e.g. originating from different properties of cloud condensation nuclei (CCN).

A first approach to include some properties of different cloud types had already been undertaken by Berry (1968). His conversion formula has often been interpreted as an autoconversion rate. However, as has been discussed by Beheng and Doms (1986) as well as Beheng (1994) the relation Berry presented cannot unambiguously be attributed to autoconversion only but has also contributions by accretion and selfcollection as one deduces from his definition of the intrinsic time scale.

Nevertheless, the idea of a partition of water mass into a cloud portion and a rain portion was a clue for further investigations leading to advanced formulations of related collection processes.

A first step towards an exact formulation of cloud microphysical parameterizations has been done by Beheng and Doms (1986) as well as Doms and Beheng (1986) in defining the partial collection mechanisms selfcollection of cloud droplets and raindrops, autoconversion and accretion for any moment of the size distributions in terms of the stochastic collection equation (SCE). Comparisons of numerical results obtained by, on one hand, a spectral approach and, on the other hand, by application of Berry's and Kessler's schemes showed a considerable disagreement, which could be traced back to the inability of both parameterization schemes to treat different cloud droplet spectra. An early attempt to consider the cloud droplet number concentration in a Kessler-type scheme has been presented by Manton and Cotton (1977) expressing Kessler's mixing ratio threshold as a function of the mean cloud droplet radius. Later, a new formulation has been suggested by Beheng (1994), who applied a two-moment approach to collisional growth of cloud droplets and raindrops. His parameterization consists of time rates of change of number densities and mass densities derived from a heuristic ansatz. Since especially the corresponding autoconversion rate depends, besides a width parameter, on both mass and number densities of cloud droplets changing simultaneously with time this scheme better represented the evolution of different droplet spectra and their influence on subsequent collection processes. However, Beheng's autoconversion rate still suffers from a strong disagreement as compared to that calculated by the spectral method. This shortcoming has been removed by Seifert and Beheng (2001, henceforth referred to as SB) by a more detailed theoretical study. They derived analytical approximations for autoconversion and accretion from the SCE itself based on the collection kernel parameterization by Long (1974) and, in addition, considering a dynamic similarity theory to parameterize the inherent time evolution of the drop size distribution.

So far this review has concentrated on collection mechanisms operating in warm clouds. However, in extra-tropical regions most clouds are mixed-phase clouds, i.e., they consist of a mixture of supercooled water and ice particles. Thus, for use in cloud resolving models a parameterization of processes taking place between (several) ice crystal types and cloud droplets as well as raindrops has to be developed. Also in this case a spectral approach is possible which again is too costly for most applications.

In the past several parameterizations have been proposed showing a different degree of complexity. Most of these schemes operate with time rates of change of mass densities only, which

later on have been completed by consideration of number densities.

In case of mass density parameterizations Wisner et al (1972) adopted Kessler's scheme and added hail growth. Cotton et al (1982), Lin et al (1983) as well as Rutledge and Hobbs (1984) took into account ice and snow as well as graupel or hail.

The first attempt dealing with number concentrations of cloud droplets, raindrops and hail goes back to the pioneering work of Ziegler (1985), who, however, restricted himself to a kinematic retrieval method. Nearly at the same time Cotton et al (1986) introduced the number density of ice crystals in a dynamic cloud model.

Almost complete two-moment parameterizations have been developed by Ferrier (1994), Meyers et al (1997) and Reisner et al (1998), who consider number and mass concentrations for all ice particle types. In some case studies these two-moment schemes have shown a better modeling and forecast skill compared with the one-moment Lin-type schemes (cf. Tao et al, 2003). But since in the schemes mentioned above the number concentration of cloud droplets is still not an independent model variable, these parameterizations are not yet suitable to study CCN effects on cloud and precipitation formation. To overcome this deficiency Feingold et al (1998) suggested a two-moment warm phase scheme, which is to a large extend based on pre-calculated look-up tables. The current version of RAMS uses this approach within the Meyers et al (1997) scheme to be suitable for investigating aerosol effects on cloud formation (Cotton et al, 2003)[1].

Here we present a consistent two-moment cloud microphysical scheme which entirely operates with rate equations for five hydrometeor types in terms of number as well as mass densities, including a full treatment of cloud droplet number concentration.

This parameterization is especially designed for use in high-resolution cloud-resolving models (CRMs) and considers CCN effects on cloud formation.

The paper is organized as follows: Sect. 2 describes the treatment of warm phase microphysical processes between cloud droplets and raindrops and includes a formulation of cloud droplets' nucleation which depends on specific aerosol types. In Sect. 3, the parameterizations are presented concerning the ice phase processes where three ice particle types, namely cloud ice, snow flakes and graupel, are distinguished. Note that the current version does not yet include a detailed description of hail-formation. Part 2 of this paper is dedicated to numerical results obtained by applying the new scheme in the framework of a limited-area atmospheric model based on compressible equations. Especially, the dynamics of mixed-phase thunderstorms in a sheared background flow is investigated and the different findings for maritime as well as continental conditions are compared with results of the classical paper of Weisman and Klemp (1982).

Note that throughout the paper some common quantities (e.g., the diffusivity of water vapour, denoted by D_v) are not addressed in detail but given in the Appendix. Numerical values are given in SI-units, except where it seems appropriate for better readability to use other units.

2. Warm phase processes

2.1 General remarks

Even in mid-latitudes warm phase processes involving water drops play a major role in precipitation formation not only due to their own contribution to surface precipitation but, maybe more important, as a prerequisite of subsequently ongoing ice phase processes.

Most important is the formation and growth of cloud droplets and raindrops by the chain of mechanisms nucleation, condensation and collection. Large raindrops originating from coalescence growth or from melting of large graupel or hail might be disrupted into smaller fragments by collisional breakup or start to evaporate as soon as they reach subsaturated regions by advection or sedimentation.

In the following paragraphs the parameterizations of all warm phase processes are described based on a decomposition of the drop size distribution into a cloud droplet and raindrop portion. The theoretical treatment follows the philosophy of Beheng and Doms (1986), Doms and Beheng (1986) as well as SB. The basic

[1] See also http://rams.atmos.colostate.edu/mexicoarticle.html

microphysical variables considered in the new scheme are the partial power moments

$$M_c^k = \int_0^{x^*} x^k f_w(x)\,dx = \int_0^{\infty} x^k f_c(x)\,dx, \tag{1}$$

$$M_r^k = \int_{x^*}^{\infty} x^k f_w(x)\,dx = \int_0^{\infty} x^k f_r(x)\,dx \tag{2}$$

of the number density size distribution function of droplets $f_w(x)$ depending on drop mass x. The drop mass x^* separates cloud droplets from raindrops and is given a value $x^* = 2.6\times10^{-10}\,\mathrm{kg}$ corresponding to a radius of $r^* = 40\,\mu\mathrm{m}$. This value has been derived from results numerically solving the stochastic collection equation.

In Eqs. (1) and (2), it has been supposed that the whole drop size spectrum can be partitioned into two discontinuous functions, $f_c(x)$ and $f_r(x)$, which are the size distribution functions of cloud droplets and raindrops, respectively. The first two partial moments of $f_w(x)$ are the number densities of cloud droplets and raindrops $M_c^0 \equiv N_c$ and $M_r^0 \equiv N_r$ as well as their mass densities (liquid water contents) $M_c^1 \equiv L_c$ and $M_r^1 \equiv L_r$. Generally it is assumed that the partial size distributions $f_c(x)$ or $f_r(x)$ can almost always be described by generalized Γ-distributions with two time dependent and two constant parameters (see Appendix A).

In Cartesian physical space $(\vec{r}, t)$ the budget equations for the partial moments $M_i^k = M_i^k(\vec{r}, t)$ with $i \in \{c, r\}$ read

$$\frac{\partial M_i^k}{\partial t} + \nabla\cdot[\vec{v} M_i^k] - \nabla\cdot[K_h \nabla M_i^k] + \frac{\partial}{\partial z}[\bar{v}_{i,k} M_i^k] = \mathcal{S}_i^k \tag{3}$$

with mean wind velocity $\vec{v}$, turbulent diffusivity of heat K_h and mean sedimentation velocities $\bar{v}_{i,k}$. In case of pure warm phase processes the source terms $\mathcal{S}_i^k$ comprise nucleation, condensation/evaporation, collision/coalescence and breakup (see below). The term $-K_h \nabla M_i^k$ is the parameterization of the turbulent fluxes of hydrometeors. Note that the moments are given in physical terms of densities rather than as mixing ratios as commonly used. The choice of a density formulation is due to two reasons: It is more straightforward in a two-moment scheme to use the densities of particle number and mass, which are simply the power moments of the size distribution $f(x)$. Moreover, this formulation makes it easier to apply a conservative flux-form advection scheme for treating the microphysical variables in a cloud model.

2.2 Coagulation and collisional breakup

To describe drop growth by collision/coalescence we apply the parameterization method developed by SB and for a detailed derivation of the rate equations for autoconversion, accretion and selfcollection from the stochastic collection equation (SCE) we refer to that paper. In contrast to SB, where in some parts the kernel approximation given by Long (1974) has been used, Seifert (2002) derived modified piecewise approximations for a kernel using collision efficiencies of Pinsky et al (2001) and, in addition, the coalescence efficiencies of Low and List (1982) and Beard and Ochs (1995). For brevity we present here the resulting parameters and equations only.

2.2.1 Autoconversion and accretion

"Autoconversion" denotes the formation of raindrops by coagulating cloud droplets whereas "accretion" terms the growth of raindrops collecting cloud droplets.

Assuming for cloud droplets a Γ-distribution with a width parameter ν_c assumed as constant and for raindrops an exponential distribution (as a function of diameter D, cf. also Appendix A) the autoconversion rate is given by (cf. SB):

$$\left.\frac{\partial L_r}{\partial t}\right|_{au} = \frac{k_{cc}}{20\,x^*}\frac{(\nu_c+2)(\nu_c+4)}{(\nu_c+1)^2} \times L_c^2 \bar{x}_c^2 \left[1 + \frac{\Phi_{au}(\tau)}{(1-\tau)^2}\right]\frac{\rho_0}{\rho} \tag{4}$$

with the dimensionless internal time scale

$$\tau = 1 - \frac{L_c}{L_c + L_r} \tag{5}$$

and $k_{cc} = 4.44\times10^9\,\mathrm{m^3\,kg^{-2}\,s^{-1}}$ based on the Pinsky et al (2001) collision efficiencies. In contrast to SB, we take into account a correction to the autoconversion rate due to the increase of the terminal fall velocity with decreasing air density (relative to surface conditions where $\rho_0 = 1.225\ \mathrm{kg\,m^{-3}}$). Similar corrections are also included in the accretion and selfcollection rates,

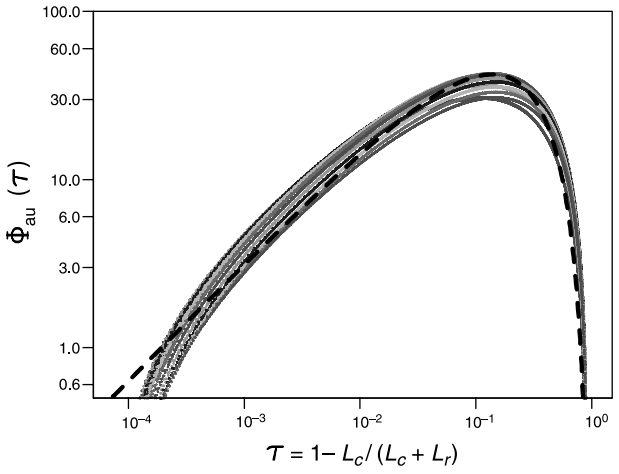

Fig. 1. Scatterplot of the numerical results for the universal autoconversion function $\Phi_{au}(\tau)$ as function of internal time scale τ as well as the curve according to Eq. (6) (thick dashed); all quantities in dimensionless units

respectively (see below). Compared to SB the consideration of an improved collection kernel mentioned above results also in slightly different similarity function $\Phi_{au}(\tau)$ given as

$$\Phi_{au}(\tau) = 400\,\tau^{0.7}(1-\tau^{0.7})^3. \tag{6}$$

This function is shown together with the numerical data gained from various explicit solutions of the SCE applying different initial drop size spectra in Fig. 1. Note that the autoconversion factor k_{cc} is by a factor of two smaller than the corresponding value originally given by Long (1974). Following Pinsky et al (2000) and Vohl et al (1999) a modification of the kernel due to turbulence effects should also be taken into account. Estimating these effects for a turbulent dissipation of $\varepsilon = 100\,\mathrm{m^2\,s^{-3}}$ similar to Table 1 of Pinsky and Khain (2002) a value of $k'_{cc} = 10.6\times10^9\,\mathrm{m^3\,kg^{-2}\,s^{-1}}$ results. As soon as the long standing problems of an explanation of droplet spectrum broadening and of the impact of turbulence on collisional growth come to a solution, the autoconversion factor k_{cc} should be formulated as a function of the turbulent dissipation ε or other parameters.

The corresponding accretion rate resulting from application of the improved kernel is given by

$$\left.\frac{\partial L_r}{\partial t}\right|_{ac} = k_{cr}\,L_c\,L_r\,\Phi_{ac}(\tau)\left(\frac{\rho_0}{\rho}\right)^{\frac{1}{2}} \tag{7}$$

with $k_{cr} = 5.25\,\mathrm{m^3\,kg^{-1}\,s^{-1}}$ and

$$\Phi_{ac}(\tau) = \left(\frac{\tau}{\tau + 5\times10^{-5}}\right)^4. \tag{8}$$

2.2.2 Selfcollection

By "selfcollection" the mechanism of cloud droplets (raindrops) by mutual coagulation but remaining in the same drop category is termed. Following SB selfcollection of cloud droplets can be expressed by

$$\left.\frac{\partial N_c}{\partial t}\right|_{sc} = -k_{cc}\frac{(\nu+2)}{(\nu+1)}\frac{\rho_0}{\rho}L_c^2 - \left.\frac{\partial N_c}{\partial t}\right|_{au}. \tag{9}$$

Regarding raindrops an improvement relative to SB has been introduced by Seifert (2002). It relies on a better representation of the terminal fall speed compared to Long's collection kernel formula. The approximate kernel for large droplets then reads

$$K_{rr}(x,y) \cong k_{rr}(x+y)\exp[-\kappa_{rr}(x^{1/3}+y^{1/3})], \qquad x,y>x^* \tag{10}$$

with $k_{rr} = 7.12\,\mathrm{m^3\,kg^{-1}\,s^{-1}}$ and $\kappa_{rr} = 60.7\,\mathrm{kg^{-1/3}}$. Assuming an exponential distribution for raindrops (as function of diameter D) this results in a selfcollection rate reading

$$\left.\frac{\partial N_r}{\partial t}\right|_{sc} = k_{rr}\,N_r\,L_r\left(1+\frac{\kappa_{rr}}{\lambda_r}\right)^{-9}\left(\frac{\rho_0}{\rho}\right)^{\frac{1}{2}}. \tag{11}$$

2.2.3 Collisional breakup

Collisional breakup has not been parameterized by SB, but can be an important process in strong precipitation and deep convective clouds. Ultimately, this process leads to the formation of the coalescence-breakup equilibrium and the corresponding self-similar equilibrium size distribution of raindrops (see, e.g., Hu and Srivastava, 1995, for a review). As shown by List (1988) and others this self-similarity reduces the complexity of the system dramatically and the equilibrium size distribution for a certain rainwater content L_r can be formulated as

$$f_{eq}(x) = L_r\,\psi_{eq}(x) \tag{12}$$

with a universal size distribution $\psi_{eq}(x)$. In a two-moment scheme collisional breakup is sim-

ply a production term for the number concentration of raindrops and the equilibrium size distribution is uniquely characterized by an equilibrium mean size of the raindrop ensemble. Due to these facts, the combined action of collisional breakup and selfcollection can be parameterized as a simple relaxation to this equilibrium mean diameter. Thus, the production of raindrops by breakup can be coupled to the selfcollection rate by the parameterization

$$\left.\frac{\partial N_r}{\partial t}\right|_{br} = -[\Phi_{br}(\Delta\bar{D}_r) + 1]\left.\frac{\partial N_r}{\partial t}\right|_{sc}, \qquad (13)$$

where $\Delta\bar{D}_r = \bar{D}_r - \bar{D}_{eq}$, with the mean volume raindrop diameter $\bar{D}_r$ and the constant equilibrium diameter $\bar{D}_{eq}$. The breakup function $\Phi_{br}(\Delta\bar{D}_r)$ is monotonically increasing with $\Phi_{br}(0) = 0$ at $\bar{D}_r = \bar{D}_{eq}$ corresponding to coalescence-breakup equilibrium. To estimate $\Phi_{br}(\Delta\bar{D}_r)$ we use a spectral model originally developed by Mayer (2000), which explicitly solves the stochastic coagulation-breakup equation based on the breakup parameterizations of Low and List (1982) as well as Beard and Ochs (1995). Using the spectral bin model several simulations with different initial conditions have been performed and as a result it turned out that the equilibrium diameter has a value of $\bar{D}_{eq} = 0.9\times10^{-3}$ m, which corresponds well with observations by Zawadzki and Agostinho (1988) in tropical rain. In the diameter range $0.35\times10^{-3}\,\mathrm{m} \le \bar{D}_r \le \bar{D}_{eq}$ the function $\Phi_{br}(\Delta\bar{D}_r)$ can be parameterized by a linear relation

$$\Phi_{br}(\Delta\bar{D}_r) = k_{br}\Delta\bar{D}_r \qquad (14)$$

with $k_{br} = 1000\,\mathrm{m}^{-1}$ and $\Delta\bar{D}_r$ in m (see Fig. 2), while for larger mean diameters ($\bar{D}_r > 0.9\times10^{-3}$ m) we assume a stronger increase and adapt the exponential relation given by Verlinde and Cotton (1993) reading

$$\Phi_{br}(\Delta\bar{D}_r) = 2\exp(\kappa_{br}\,\Delta\bar{D}_r) - 1, \qquad (15)$$

where $\kappa_{br} = 2.3\times10^3\,\mathrm{m}^{-1}$. For $\bar{D}_r < 0.35\times10^{-3}$ m breakup is neglected, i.e., $\Phi_{br}(\Delta\bar{D}_r) = -1$.

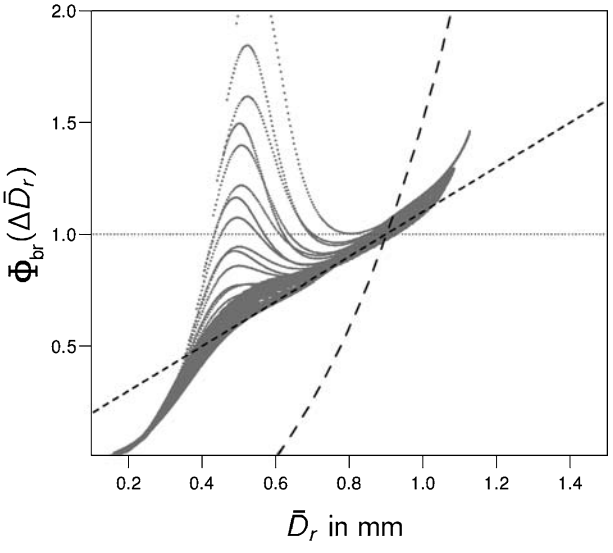

Fig. 2. Scatterplot of the numerical results for the dimensionless breakup function $\Phi_{br}(\Delta\bar{D}_r)$ as function of the mean volume raindrop diameter $\bar{D}_r$ as well as curves according to Eq. (14) (short dashed) and Eq. (15) (long dashed)

2.3 Nucleation and condensation

2.3.1 Nucleation of cloud droplets

In a cloud scheme applying a two-moment approach to the cloud droplet ensemble (thus taking N_c as a time dependent model variable) nucleation of cloud droplets has to be treated explicitly. Recently Cohard et al (1998), and Cohard et al (2000) suggested a sophisticated nucleation parameterization based on the so-called Twomey equations suitable for two-moment schemes. Unfortunately, the extension of this scheme to mixed-phase clouds is not straightforward.

Therefore a more direct technique is used which is based on grid scale supersaturation. This seems to be appropriate here since the scheme will be applied in an atmospheric model with a horizontal grid size of $\Delta x \le 1$ km and a small time step $\Delta t < 10$ s, which decreases to $\Delta t \approx 1$ s in case of strong updrafts.

To describe the aerosol activation without an explicit calculation of Köhler-Kelvin theory the parameterization is based on empirical activation spectra in form of a power law relation

$$N_{\mathrm{ccn}}(S) = C_{\mathrm{ccn}}\,S^{\kappa}, \quad S \text{ in } \% \qquad (16)$$

with $C_{\mathrm{ccn}} = 1.26\times10^9\,\mathrm{m}^{-3}$ and $\kappa = 0.308$ for continental conditions or $C_{\mathrm{ccn}} = 1.0\times10^8\,\mathrm{m}^{-3}$ and $\kappa = 0.462$ for maritime conditions (Khain et al, 2001). In case of maritime CCN we assume that at $S_{\max} = 1.1\%$ all CCN are al-

ready activated and no further activation takes place.

Accordingly, at grid points with positive supersaturation S we calculate an explicit nucleation rate following from time differentiation of the activation relation:

$$\left.\frac{\partial N_c}{\partial t}\right|_{\text{nuc}} = \begin{cases} C_{\text{ccn}}\,\kappa S^{\kappa-1}\dfrac{\partial S}{\partial z}w, & \text{if } S \geq 0,\ w\dfrac{\partial S}{\partial z} > 0 \\ & \text{and } S < S_{\max} \\ 0, & \text{else,} \end{cases} \tag{17}$$

$$\left.\frac{\partial L_c}{\partial t}\right|_{\text{nuc}} = x_{c,\text{nuc}}\left.\frac{\partial N_c}{\partial t}\right|_{\text{nuc}}, \tag{18}$$

where $x_{c,\text{nuc}} = 1\times10^{-12}\,\text{kg}$ is an arbitrarily chosen smallest drop mass. To simplify the evaluation of the scheme in a 3-D Eulerian model dS/dt is approximated by $w\,\partial S/\partial z$, assuming that activation is dominated by vertical motions.

In the current version of this scheme no balance equation for aerosol particles is considered in the parameterization and it is therefore necessary to limit the absolute number of activated particles (or cloud droplets, respectively). As limiting concentrations we chose $150\times10^6\,\text{m}^{-3}$ in the maritime case and $1500\times10^6\,\text{m}^{-3}$ for continental conditions.

2.3.2 Condensational growth of cloud droplets

As shown by Kogan and Martin (1994) all clouds, except extremely maritime ones, relax rapidly to the thermodynamic equilibrium between water vapor and water drops. Thus, applying the standard saturation adjustment technique to treat condensational growth seems to be appropriate in almost all cases. It is clearly paradox to use a nucleation scheme explicitly depending on supersaturation in combination with a saturation adjustment which removes instantaneously all supersaturations. But since we apply an operator splitting method (cf. part 2 of this paper, pp 67–82) to treat these processes numerically, this is possible and, as long as no better general and efficient combined nucleation/condensation parameterization for mixed-phase clouds is available, this efficient and robust approach can be used in practice.

2.4 Sedimentation

Obviously sedimentation, especially of raindrops, is crucial for a quantitative modeling of surface precipitation. The straightforward approach to consider sedimentation in a two-moment scheme based on number ($k = 0$) and mass densities ($k = 1$) is to use corresponding number and mass weighted mean fall velocities:

$$\begin{aligned}\bar{v}_{r,k} &= \frac{1}{M_r^k}\int_{x^*}^{\infty} x^k f_w(x) v_w(x)\,dx \\ &\cong \frac{1}{M_r^k}\int_{0}^{\infty} x^k f_w(x) v_w(x)\,dx.\end{aligned} \tag{19}$$

To approximate the individual terminal fall velocity of drops $v_w(x)$ we apply an empirical relation similar to Rogers et al (1993), but including an increase of the terminal fall velocity with height:

$$v_w \cong \left(\frac{\rho_0}{\rho}\right)^{\frac{1}{2}}\left[a_R - b_R e^{-c_R D_r}\right] \tag{20}$$

with $a_R = 9.65\,\text{m s}^{-1}$, $b_R = 10.3\,\text{m s}^{-1}$ and $c_R = 600\,\text{m}^{-1}$. Again we assume an exponential size distribution (as function of diameter, see Appendix A) for the raindrop ensemble. After integrating Eq. (20) from 0 to ∞ we arrive at an equation for the weighted fall velocity reading

$$\bar{v}_{r,k} = \left(\frac{\rho_0}{\rho}\right)^{\frac{1}{2}}\left[a_R - b_R\left(1 + \frac{c_R}{\lambda_r}\right)^{-(3k+1)}\right]. \tag{21}$$

Unfortunately, the application of this straightforward parameterization can lead to artifacts arising from the nonlinearity, which enters the sedimentation equation when the drop size variable itself is eliminated. This occurs in every one- or two-moment scheme as shown by Wacker and Seifert (2001). To overcome these problems we suggest to limit the slope and the intercept of the assumed exponential distribution (see Appendix D). This cannot eliminate the nonlinear shock-waves, which are an inherent property of the parameterized sedimentation equations, but at least limits the speed of the shock-waves resulting in a much better description of the overall rainrate.

Sedimentation of cloud droplets is described using the same approach, but based on considering Stokes' terminal fall velocity and a generalized Γ-distribution.

2.5 Evaporation of raindrops

Following Pruppacher and Klett (1997) evaporation of a single raindrop of mass x_r with diameter $D_r(x_r)$ can be described by

$$\left.\frac{dx_r}{dt}\right|_{\text{eva}} = 2\pi\, D_r(x_r)\, G_{lv}(T,p)\, F_v(x_r)\, S \tag{22}$$

with

$$G_{lv}(T,p) = \left[\frac{R_v T}{p_{lv}(T) D_v} + \frac{L_{lv}}{K_T T}\left(\frac{L_{lv}}{R_v T} - 1\right)\right]^{-1} \tag{23}$$

and a ventilation factor given by

$$F_v = a_v + b_v N_{Sc}^{1/3} N_{Re}^{1/2} \tag{24}$$

comprising two constants $a_v = 0.78$, $b_v = 0.308$ and the Reynolds as well as the Schmidt number. We assume the latter to be constant with $N_{Sc} = \nu_a / D_v = 0.71$, which is a typical value for the atmosphere. The Reynolds number of a single raindrop falling is given by

$$N_{Re}(x) = \frac{v_r(x) D_r(x)}{\nu_{\text{air}}}. \tag{25}$$

To derive a parameterization equation for the n-th moment of the raindrop size distribution we apply an approach similar as described by Murakami (1990) in his parameterization of the conversion of graupel to snow. Thus, we start by estimating the characteristic time for evaporation of a raindrop by

$$\tau_{\text{eva}} = \frac{x_r}{\left.\frac{dx_r}{dt}\right|_{\text{eva}}} = \frac{1}{2\pi\, G_{lv}(T,p)\, S} \frac{x_r}{D_r(x_r)\, F_v(x_r)} \tag{26}$$

and arrive at an equation for the rate of change of the power moments reading

$$\begin{aligned}\left.\frac{\partial M_r^n}{\partial t}\right|_{\text{eva}} &= \int_0^\infty \frac{x^n f_r(x)}{\tau_{\text{eva}}} dx \\ &= 2\pi G_{lv}(T,p) S \int_0^\infty D_r(x) F_v(x) f_r(x) x^{n-1} dx.\end{aligned} \tag{27}$$

To simplify integration we assume a terminal fall velocity in form of a power law instead of Eq. (20) given by

$$v_r(x) \cong \alpha_r x^{\beta_r} \left(\frac{\rho_0}{\rho}\right)^{\frac{1}{2}} \tag{28}$$

with $\alpha = 159\,\text{m}\,\text{s}^{-1}\,\text{kg}^{-\beta_r}$ and $\beta_r = 2/3$. Using a generalized Γ-distribution to parameterize $f_r(x)$, which includes the exponential distribution depending on D (see Appendix A), the integral can be evaluated analytically. After a lengthy, but straightforward calculation this yields

$$\left.\frac{\partial M_r^n}{\partial t}\right|_{\text{eva}} = 2\pi\, G_{lv}(T,p)\, S N_r\, D_r(\bar{x}_r)\, \bar{F}_{v,n}(\bar{x}_r)\, \bar{x}^{n-1}, \tag{29}$$

wherein $\bar{F}_{v,n}$ is an averaged ventilation factor for n-th power moment of the raindrop ensemble given by

$$\bar{F}_{v,n}(\bar{x}_r) = \bar{a}_{\text{vent},n} + \bar{b}_{\text{vent},n} N_{Sc}^{1/3} N_{Re}^{1/2}(\bar{x}_r), \tag{30}$$

with the Reynolds number of the mean raindrop

$$N_{Re}(\bar{x}_r) = \frac{v_r(\bar{x}_r) D_r(\bar{x}_r)}{\nu_{\text{air}}}, \quad \bar{x}_r = \frac{L_r}{N_r} \tag{31}$$

and constants $\bar{a}_{\text{vent},n}$ and $\bar{b}_{\text{vent},n}$, which are given in Appendix B. It is emphasized that $F_v(\bar{x}_r) \neq \bar{F}_{v,n}(\bar{x}_r)$ and, e.g. $\bar{F}_{v,0}(\bar{x}_r) \neq \bar{F}_{v,1}(\bar{x}_r)$ which leads to a change of the mean drop size during evaporation. In addition, every two-moment parameterization of the evaporation process suffers from similar problems as the sedimentation scheme, thus the limitation of slope and intercept described in Appendix D is applied here, too.

3. The ice phase scheme

3.1 General remarks

The ice phase scheme is in some parts similar to the MM5 two-moment scheme described by Reisner et al (1998), which in turn follows the work of Cotton et al (1982), Lin et al (1983), Rutledge and Hobbs (1984), Murakami (1990) and others. The diameter-mass- as well as the velocity-mass-relations of the different particles are parameterized by power laws

$$D(x) \cong a\, x^b, \tag{32}$$

$$v(x) \cong \alpha\, x^\beta \left(\frac{\rho_0}{\rho}\right)^\gamma \tag{33}$$

with constant coefficients a, b, α, β and γ, which are summarized in Table 1. For non-spherical particles $D(x)$ is defined as the maximum dia-

Table 1. Power law coefficients for the maximum diameter $D(x)$ and the terminal fall velocity $v(x)$ of particles with mass x as well as coefficients of the generalized Γ-distribution for the various hydrometeor types as used in the present scheme. The geometries and fall velocities of ice particles are based on measurements of Locatelli and Hobbs (1974) and Heymsfield and Kajikawa (1987)

	a ($\mathrm{m\,kg^{-\beta}}$)	b	α ($\mathrm{m\,s^{-1}\,kg^{-\beta}}$)	β	γ	ν	μ	$\bar{x}_{\min}$ (kg)	$\bar{x}_{\max}$ (kg)
cloud droplets	0.124	1/3	3.75×10^{5}	2/3	1	1	1	4.20×10^{-15}	1.00×10^{-11}
raindrops	0.124	1/3	159.0	0.266	1/2	−2/3	1/3	2.60×10^{-10}	5.00×10^{-6}
cloud ice	0.217	0.302	317.0	0.363	1/2	1	1/3	1.00×10^{-12}	1.00×10^{-7}
snowflakes	8.156	0.526	27.7	0.216	1/2	1	1/3	1.73×10^{-9}	1.00×10^{-7}
graupel	0.190	0.323	40.0	0.230	1/2	1	1/3	2.60×10^{-10}	1.00×10^{-4}

meter as given by Locatelli and Hobbs (1974) or Heymsfield and Kajikawa (1987). For cloud ice the "hexagonal plates" of Heymsfield and Kajikawa (1987) have been chosen, snowflakes are described as "mixed aggregates" of Locatelli and Hobbs (1974) and for graupel the "lump graupel" geometry of Heymsfield and Kajikawa (1987) is used describing low density particles. The fall velocity of graupel has been fitted to a calculation based on the approach of Heymsfield and Kajikawa (1987). As described in the previous section and in Appendix A generalized Γ-distributions with constant coefficients ν and μ are used to describe the various size distributions. To avoid unrealistic large or small mean masses in the parameterization upper and lower limits are applied to the mean mass $\bar{x} = L/N$ of the particles. For the five different particle types used in the present scheme these coefficients are summarized in Table 1.

3.2 Nucleation of cloud ice

To parameterize the nucleation of small ice particles we follow Reisner et al (1998) and others and apply a number density adjustment reading

$$\left.\frac{\partial N_i}{\partial t}\right|_{\mathrm{nuc}} = \begin{cases} \dfrac{N_{IN}(S_i,T) - N_i}{\Delta t}, & \text{if } S_i \geq 0 \text{ and } N_i < N_{IN}(S_i,T) \\ 0, & \text{else} \end{cases} \tag{34}$$

$$\left.\frac{\partial L_i}{\partial t}\right|_{\mathrm{nuc}} = x_{i,\mathrm{nuc}} \left.\frac{\partial N_i}{\partial t}\right|_{\mathrm{nuc}}, \tag{35}$$

where $x_{i,\mathrm{nuc}} = 1\times10^{-12}\,\mathrm{kg}$ is the minimum mass of ice particles in the present scheme. Alternatively ice nucleation could be treated similar to the cloud droplet nucleation using an explicit nucleation rate as a function of the updraft velocity. As parameterization of the number of ice nuclei we apply the deposition-condensation nucleation formula as given by Meyers et al (1992):

$$N_{IN} = N_{\mathrm{M92}} \exp[a_{\mathrm{M92}} + b_{\mathrm{M92}} S_i], \tag{36}$$

where $N_{\mathrm{M92}} = 1\times10^{3}\,\mathrm{m^{-3}}$ and $a_{\mathrm{M92}} = -0.639$, $b_{\mathrm{M92}} = 12.96$.

In order to avoid very low number concentrations we limit the deviations of the ice crystal number density from the modified Fletcher-formula as given by Reisner et al (1998) to one order in magnitude.

3.3 Growth of ice particles by water vapor deposition

Depositional growth of a single ice particle (cloud ice, snow, graupel) can be described using the following general growth equation (cf. Cotton et al, 1986; Pruppacher and Klett, 1997)

$$\left.\frac{dx_i}{dt}\right|_{\mathrm{dep}} = \frac{4\pi C_i F_v(x_i) S_i}{\dfrac{R_v T}{p_{iv}(T) D_v} + \dfrac{L_{iv}}{K_T T}\left(\dfrac{L_{iv}}{R_v T} - 1\right)} = \frac{4\pi}{c_i} D_i\, G_{iv}(T,p)\, F_v(x_i)\, S_i \tag{37}$$

with

$$G_{iv}(T,p) = \left[\frac{R_v T}{p_{iv}(T) D_v} + \frac{L_{iv}}{K_T T}\left(\frac{L_{iv}}{R_v T} - 1\right)\right]^{-1}, \tag{38}$$

where $C_i = D_i/c_i = D_i/2$ is the capacity of spherical particles. For hexagonal plates the approximation $C_i \approx D_i/\pi$ is used (cf. Harrington et al,

1995). Integration results in an equation for the mass density of a particle ensemble

$$\left.\frac{\partial L_i}{\partial t}\right|_{\text{dep}} = \int_0^\infty \left.\frac{dx_i}{dt}\right|_{\text{dep}} f_i(x)\,dx = \frac{4\pi}{c_i} G_{iv}(T,p)\,S_i \int_0^\infty D_i(x) F_v(x) f_i(x)\,dx. \tag{39}$$

The ventilation coefficient $F_v(x)$ for spherical particles is given by

$$F_v = a_{v,i} + b_{v,i} N_{Sc}^{1/3} N_{Re}^{1/2} \tag{40}$$

with $a_v = 0.78$ and $b_v = 0.308$, the Schmidt number $N_{Sc} = 0.71$ and the Reynolds number N_{Re} (Pruppacher and Klett, 1997). Based on the results of Hall and Pruppacher (1976) $a_v = 0.86$ and $b_v = 0.28$ can be used for thin plates. The Reynolds number of a single ice particle falling with terminal fall velocity v_i is given by

$$N_{Re}(x) = \frac{v_i(x) D_i(x)}{\nu_{\text{air}}}, \qquad v_i(x_i) \cong \alpha_i x_i^{\beta_i} \left(\frac{\rho_0}{\rho}\right)^{\frac{1}{2}}. \tag{41}$$

Assuming a generalized Γ-distribution for $f_i(x)$ the integration results in

$$\left.\frac{\partial L_i}{\partial t}\right|_{\text{dep}} = \frac{4\pi}{c_i} G_{iv}(T,p)\; D_i(\bar{x})\, \bar{F}_{v,1}\, S_i \tag{42}$$

with the averaged ventilation coefficient (see Appendix B)

$$\bar{F}_{v,1} = \bar{a}_{\text{vent},1} + \bar{b}_{\text{vent},1}\, N_{Sc}^{1/3}\, N_{Re}^{1/2}(\bar{x}_i). \tag{43}$$

3.4 Freezing of water drops

Following the classical work of Bigg (1953) we describe heterogenous freezing of raindrops by a stochastical model. The relative time rate of change of the size distribution by heterogenous freezing is given by (cf. Khain et al, 2000)

$$\left.\frac{1}{f_r(x)}\frac{\partial f_r(x)}{\partial t}\right|_{\text{het}} = -x\, A_{\text{het}}\, \exp[B_{\text{het}}(T_3 - T) - 1] = -x\, J_{\text{het}}(T) \tag{44}$$

and the parameters are set to $A_{\text{het}} = 0.2\,\text{kg}^{-1}\,\text{s}^{-1}$ and $B_{\text{het}} = 0.65\,\text{K}^{-1}$ (Pruppacher and Klett, 1997). The corresponding moment equations are then given by

$$\left.\frac{\partial M_w^k}{\partial t}\right|_{\text{het}} = -M_w^{k+1}\, J_{\text{het}}(T). \tag{45}$$

To close these coupled equations an exponential distribution is assumed for $f_r(D)$ (see Appendix A) resulting in:

$$\left.\frac{\partial N_r}{\partial t}\right|_{\text{het}} = -L_r\, J_{\text{het}}(T) = -N_r\, \bar{x}_r\, J_{\text{het}}(T), \tag{46}$$

$$\left.\frac{\partial L_r}{\partial t}\right|_{\text{het}} = -Z_r\, J_{\text{het}}(T) = -20\, L_r\, \bar{x}_r\, J_{\text{het}}(T). \tag{47}$$

Here Z_r denotes the second moment of $f_r(x)$, which is proportional to the 6-th moment of $f_r(D)$ with the radar cross section in Rayleigh approximation.

Heterogenous freezing of cloud droplets is treated similarly, but closure is then reached by assuming a Γ-distribution for $f_c(x)$.

Homogenous freezing of cloud droplets is parameterized following Jeffrey and Austin (1997) and Cotton and Field (2002) by

$$\left.\frac{1}{f_c(x)}\frac{\partial f_c(x)}{\partial t}\right|_{\text{hom}} = -x\, J_{\text{hom}}(T) \tag{48}$$

with $J_{\text{hom}}(T)$ given by Eq. (3) of Cotton and Field (2002). Assuming a Γ-distribution for $f_c(x)$ yields:

$$\left.\frac{\partial N_c}{\partial t}\right|_{\text{hom}} = -L_c\, J_{\text{hom}}(T) = -N_c\, \bar{x}_c\, J_{\text{hom}}(T), \tag{49}$$

$$\left.\frac{\partial L_c}{\partial t}\right|_{\text{hom}} = -Z_c\, J_{\text{hom}}(T) = -\frac{\nu_c + 2}{\nu_c + 1}\, L_c\, \bar{x}_c\, J_{\text{hom}}(T). \tag{50}$$

Homogenous freezing of raindrops can be omitted, since raindrops freeze rapidly by heterogenous freezing and do not reach the level of homogenous freezing.

3.5 Collection processes

The various collection processes, e.g., aggregation, and related secondary processes, like ice multiplication, are summarized in Table 2. This table contains also the warm phase coagulation processes.

3.5.1 Collision integrals

To overcome some deficiencies of commonly used formulas and to avoid look-up tables for

Table 2. Interactions between hydrometeors including secondary processes like enhanced melting or Hallett-Mossop ice multiplication. (RH84 = Rutledge and Hobbs, 1984, B82 = Beheng, 1982)

	cloud droplets	raindrops	ice crystals	snowflakes
cloud droplets	selfcollection: $c + c \rightarrow c$ (Eq. 9) autoconversion: $c + c \rightarrow r$ (Eqs. 4–6)			
raindrops	accretion: $r + c \rightarrow r$ (Eqs. 7–8)	selfcollection: $r + r \rightarrow r$ (Eqs. 10–11) breakup: $r + r \rightarrow r$ (Eqs. 13–15)		
ice crystals	riming: $i + c \rightarrow i$ (Eqs. 61–67)	riming to gaupel: $r + i \rightarrow g$ (similar to Eqs. 61–63, with $\bar{E}_{ir} = 1$)	aggregation to snow: $i + i \rightarrow s$ (similar to Eqs. 61–67)	
	conversion to graupel: $i + c \rightarrow g$ (Eqs. 70–71, with $\alpha_{\circ,\mathrm{ice}} = 0.68$)	enhanced melting: Eq. (A21) of RH84		
	enhanced melting: Eq. (A22) of RH84			
	ice multiplication: $i + c \rightarrow i$ Eq. (7) of B82			
snowflakes	riming: $s + c \rightarrow i$ (Eqs. 61–67)	riming to graupel: $r + s \rightarrow g$ (similar to Eqs. 61–63, with $E_{sr} = 1$)	aggregation: $i + s \rightarrow s$ (Eqs. 61–67)	aggregation: $s + s \rightarrow s$ (Eqs. 61–67)
	conversion to graupel: $s + c \rightarrow g$ (as Eqs. 70–71, with $\alpha_{\circ,\mathrm{snow}} = 0.01$)	enhanced melting: Eq. (A21) of RH84		
	enhance melting: Eq. (A22) of RH84			
	ice multiplication: $s + c \rightarrow i$ Eq. (7) of B82			
graupel	riming: $g + c \rightarrow g$ (Eqs. 61–67)	riming: $r + g \rightarrow g$ (Eqs. 61–63, with $E_{gr} = 1$)	zero efficiency	aggregation: $s + g \rightarrow g$ (Eqs. 61–67)
	enhanced melting: Eq. (A22) of RH84	enhanced melting: Eq. (A21) of RH84		
	ice multiplication: $g + c \rightarrow i$ Eq. (7) of B82			

numerically pre-calculated integrals an improved approximation to the integrals describing collisional interaction between arbitrary particles is proposed. For example, the evolution of the power moments M^k of two interacting particle ensembles where "a" collects "b" to form larger particles of type "a" can be described by

$$\left.\frac{\partial M_a^k}{\partial t}\right|_{\mathrm{coll},ab} = + \int_0^\infty \int_0^\infty f_a(x) f_b(y)\, K_{ab}(x,y) \times [(x+y)^k - y^k]\, dx\, dy, \qquad (51)$$

$$\left.\frac{\partial M_b^k}{\partial t}\right|_{\text{coll},ab} = -\int_0^\infty \int_0^\infty f_a(x) f_b(y)\, K_{ab}(x,y)\, y^k dx\, dy \tag{52}$$

with the collection kernel

$$K_{ab}(x,y) = \frac{\pi}{4}[D_a(x)+D_b(y)]^2 |v_a(x)-v_b(y)| E_{ab}(x,y). \tag{53}$$

In generalizing the approach suggested by Wisner et al (1972) we assume that the integrals in Eqs. (51) and (52) can be expressed by a mean efficiency $\bar{E}_{ab}$, which depends only on the mean masses, a characteristic velocity difference $\overline{\Delta v_{ab}}$ and a purely geometric term depending on D_a and D_b. To avoid lengthy general formulas for arbitrary moments, the procedure is demonstrated regarding the mass density equation of the collector only. It then follows that

$$\left.\frac{\partial L_a}{\partial t}\right|_{\text{coll},ab} = \frac{\pi}{4}\overline{\Delta v_{ab}}\, \bar{E}_{ab}(\bar{x},\bar{y}) \int_0^\infty \int_0^\infty f_a(x) f_b(y) \times [D_a(x) + D_b(x)]^2\, y\, dx\, dy. \tag{54}$$

Assuming generalized Γ-distributions for $f_a(x)$ and $f_b(x)$ as well as power laws relating the mass x to diameter D, this integral can easily be evaluated analytically in terms of Gamma-functions. In contrast to Wisner et al (1972) and others we do not approximate $\overline{\Delta v_{ab}}$ by a simple difference of somehow averaged mean velocities, since this leads to the well known paradox of vanishing $\overline{\Delta v_{ab}}$ for polydisperse spectra, but apply the following approximation:

$$\overline{\Delta v_{ab}} = \left[\frac{1}{\mathcal{N}}\int_0^\infty \int_0^\infty [v_a(x) - v_b(y)]^2 D_a^2 D_b^2 f_a(x) \times f_b(y)\, y\, dx\, dy\right]^{\frac{1}{2}}, \tag{55}$$

wherein the normalization factor $\mathcal{N}$ is

$$\mathcal{N} = \int_0^\infty \int_0^\infty D_a^2 D_b^2 f_a(x) f_b(y)\, y\, dx\, dy = C_{\mathcal{N}} N_a N_b D_a^2(\bar{x}_a) D_b^2(\bar{x}_b)\, \bar{x}_a \tag{56}$$

with a constant $C_{\mathcal{N}}$. Similar to the geometric integrals in Eq. (54) this mean velocity difference can be integrated analytically if the velocity–mass relations are power laws as assumed throughout this paper (cf. Table 1). As result of this approach we then find equations for the evolution of the number and mass densities of the two particle ensembles:

$$\left.\frac{\partial L_a}{\partial t}\right|_{\text{coll},ab} = \frac{\pi}{4}\bar{E}_{ab} N_a L_b [\delta_a^0 D_a^2(\bar{x}_a) + \delta_{ab}^1 D_b(\bar{x}_b) D_a(\bar{x}_a) + \delta_b^1 D_b^2(\bar{x}_b)] \times [\vartheta_a^0 v_a^2(\bar{x}_a) - \vartheta_{ab}^1 v_b(\bar{x}_b) v_a(\bar{x}_a) + \vartheta_b^1 v_b^2(\bar{x}_b)]^{\frac{1}{2}}, \tag{57}$$

$$\left.\frac{\partial N_b}{\partial t}\right|_{\text{coll},ab} = -\frac{\pi}{4}\bar{E}_{ab} N_a N_b [\delta_a^0 D_a^2(\bar{x}_a) + \delta_{ab}^0 D_b(\bar{x}_b) D_a(\bar{x}_a) + \delta_b^0 D_b^2(\bar{x}_b)] \times [\vartheta_a^0 v_a^2(\bar{x}_a) - \vartheta_{ab}^0 v_b(\bar{x}_b) v_a(\bar{x}_a) + \vartheta_b^0 v_b^2(\bar{x}_b)]^{\frac{1}{2}}, \tag{58}$$

$$\left.\frac{\partial L_b}{\partial t}\right|_{\text{coll},ab} = -\left.\frac{\partial L_a}{\partial t}\right|_{\text{coll},ab}, \tag{59}$$

wherein the δ's and ϑ's are dimensionless constants, which depend only on the chosen size distributions and the velocity – as well as diameter – mass-relations of the particles "a" and "b" (see Appendix C).

Application of this improved Wisner-approximation to other collection processes, e.g., "a" collecting "b" to form "c" (a + b → c, cf. Table 2) or the selfcollection of particles ("a" collecting "a" and remains "a", a + a → a) is straightforward and has been given in all details by Seifert (2002).

The formulation of the mean velocity difference using the variance ansatz Eq. (55) has been inspired by a parameterization used by Murakami (1990) and Mizuno (1990). The approach can be generalized by including a probability formulation for the particle velocities. In this case the kernel itself is defined by the integral formulation

$$K_{ab}(x,y) = \int_{u=-\infty}^{+\infty}\int_{v=-\infty}^{+\infty} \frac{\pi}{4}[D_a(x)+D_b(y)]^2 \times E_{ab}(x,y) P_a(u|x) P_b(v|y) |u-v|\, du\, dv, \tag{60}$$

where the velocity distribution $P_a(u|x)$ is defined as the probability of a particle of type "a" with mass x to fall with velocity u. Assuming Gaussian distributions for P_a and P_b with means $v_a(x)$ resp. $v_b(x)$ and constant variances σ_a resp. σ_b we arrive at:

$$\begin{aligned}\left.\frac{\partial L_a}{\partial t}\right|_{\text{coll},ab} &= \frac{\pi}{4}\bar{E}_{ab}\,N_a\,L_b[\delta_a^0\,D_a^2(\bar{x}_a) \\ &+ \delta_{ab}^1\,D_b(\bar{x}_b)D_a(\bar{x}_a) + \delta_b^1\,D_b^2(\bar{x}_b)] \\ &\times[\vartheta_a^0\,v_a^2(\bar{x}_a) - \vartheta_{ab}^1\,v_b(\bar{x}_b)v_a(\bar{x}_a) \\ &+ \vartheta_b^1\,v_b^2(\bar{x}_b) + \sigma_a + \sigma_b]^{\frac{1}{2}}, \end{aligned} \tag{61}$$

$$\begin{aligned}\left.\frac{\partial N_b}{\partial t}\right|_{\text{coll},ab} &= -\frac{\pi}{4}\bar{E}_{ab}\,N_a\,N_b[\delta_a^0\,D_a^2(\bar{x}_a) \\ &+ \delta_{ab}^0\,D_b(\bar{x}_b)D_a(\bar{x}_a) + \delta_b^0\,D_b^2(\bar{x}_b)] \\ &\times[\vartheta_a^0\,v_a^2(\bar{x}_a) - \vartheta_{ab}^0\,v_b(\bar{x}_b)v_a(\bar{x}_a) \\ &+ \vartheta_b^0\,v_b^2(\bar{x}_b) + \sigma_a + \sigma_b]^{\frac{1}{2}}, \end{aligned} \tag{62}$$

$$\left.\frac{\partial L_b}{\partial t}\right|_{\text{coll},ab} = -\left.\frac{\partial L_a}{\partial t}\right|_{\text{coll},ab}. \tag{63}$$

This concept is applied to the cloud ice and snow particles with $\sigma_i = \sigma_s = 0.2\,\text{m s}^{-1}$, while zero velocity variance is assumed for cloud droplets, raindrops and graupel ($\sigma_c = \sigma_r = \sigma_g = 0$). Please note that within these equations a height correction of the terminal fall velocities is applied for all particle types.

3.5.2 Collision and sticking efficiencies

The mean collision efficiencies $\bar{E}_{ab}$ could be formulated in a similar way as the mean velocity difference by calculating properly weighted integrals of E_{ab}, but since E_{ab} itself cannot be approximated by a power law a simpler approach is applied describing the mean efficiency as a piecewise linear functions of the mean diameters. For the collection of cloud droplets by cloud ice, snow and graupel we assume ($e \in \{i, s, g\}$):

$$\bar{E}_{\text{coll},ec}(\bar{D}_e, \bar{D}_c) = \bar{E}_c(\bar{D}_c)\;\bar{E}_e(\bar{D}_e), \tag{64}$$

where

$$\bar{E}_c(\bar{D}_c) = \begin{cases} 0, & \text{if } \bar{D}_c < \bar{D}_{c,0} \\ \dfrac{\bar{D}_c - \bar{D}_{c,0}}{\bar{D}_{c,1} - \bar{D}_{c,0}} & \text{if } \bar{D}_{c,0} \le \bar{D}_c \le \bar{D}_{c,1}\,, \\ 1, & \text{if } \bar{D}_c > \bar{D}_{c,1} \end{cases} \tag{65}$$

with $\bar{D}_{c,0} = 15\,\mu\text{m}$, $\bar{D}_{c,1} = 40\,\mu\text{m}$ and

$$\bar{E}_e(\bar{D}_e) = \begin{cases} 0, & \text{if } \bar{D}_e \le \bar{D}_{e,0} \\ \bar{E}_{e,\max}, & \text{if } \bar{D}_e > \bar{D}_{e,0} \end{cases} \tag{66}$$

with $\bar{D}_{i,0} = \bar{D}_{s,0} = \bar{D}_{g,0} = 150\,\mu\text{m}$, $\bar{E}_{i,\max} = \bar{E}_{s,\max} = 0.8$ and $\bar{E}_{g,\max} = 1.0$. In this first version of the scheme we neglect the difference between mean efficiencies for number and mass densities and apply the same formulas to both moments. For all collisions between ice particles and collisions between raindrops and ice particles a mean collision efficiency of one is assumed ($\bar{E}_{\text{coll},ee} = 1$, $\bar{E}_{\text{coll},er} = 1$).

The sticking efficiencies of the snow–snow-, ice–ice-, snow–ice-, and graupel–snow-collisions are parameterized by

$$\bar{E}_{\text{stick}}(T) = \exp(0.09\,T_c) \tag{67}$$

as given by Lin et al (1983). The sticking efficiencies of graupel-ice- and graupel–graupel-collisions are assumed to be zero. Note, that the collision efficiency for drop–drop-collisions is already included in the warm phase parameterization by using approximate collision kernels (cf. Sect. 2.2).

3.5.3 Partial conversion of ice and snow to graupel

Following Beheng (1981) a riming ice crystal becomes a graupel particle as soon as the collected mass fills up the enveloping sphere, thus the sphere associated with the maximum diameter of the ice crystal. This geometric argument corresponds to a mean critical rime mass for the conversion from cloud ice to graupel reading

$$x_{\text{crit,rime}} = \alpha_\circ \rho_w \left(\frac{\pi}{6}\bar{D}_i^3 - \frac{\bar{x}_i}{\rho_\varepsilon}\right) \tag{68}$$

with the mean (maximum) diameter $\bar{D}_i$, the densities of water and ice substance $\rho_w = 1000\,\text{kg m}^{-3}$ and $\rho_\varepsilon = 900\,\text{kg m}^{-3}$ and the so-called space filling coefficient $\alpha_\circ = 0.68$. Know-

ing the riming rate $\frac{\partial L_i}{\partial t}\big|_{\text{rime}}$ the characteristic time τ_{conv} for this conversion process is calculated by (cf. Eq. (26))

$$\tau_{\text{conv}} = \frac{x_{\text{crit,rime}}}{\frac{\partial \bar{x}_i}{\partial t}\big|_{\text{rime}}} = \frac{x_{\text{crit,rime}}}{\frac{1}{N_i}\frac{\partial L_i}{\partial t}\big|_{\text{rime}}} = \frac{\alpha_\circ \rho_w N_i \left(\frac{\pi}{6}\bar{D}_i^3 - \frac{\bar{x}_i}{\rho_\varepsilon}\right)}{\frac{\partial L_i}{\partial t}\big|_{\text{rime}}}. \tag{69}$$

The conversion rate from ice to graupel due to riming (i + c → g in Table 2) is parameterized as the ratio of the mass density of the riming crystals and the characteristic conversion time:

$$\frac{\partial L_g}{\partial t}\bigg|_{\text{conv}} = \frac{L_i}{\tau_{\text{conv}}} = \frac{1}{\alpha_\circ \frac{\rho_w}{\rho_\varepsilon}\left(\frac{\frac{\pi}{6}\rho_\varepsilon \bar{D}_i^3}{\bar{x}_i} - 1\right)} \frac{\partial L_i}{\partial t}\bigg|_{\text{rime}}. \tag{70}$$

For the number concentration it is assumed

$$\frac{\partial N_g}{\partial t}\bigg|_{\text{conv}} = \frac{1}{\bar{x}_i}\frac{\partial L_g}{\partial t}\bigg|_{\text{conv}}. \tag{71}$$

To suppress the early formation of very small graupel particles conversion takes place only if the cloud ice mean diameter $\bar{D}_i$ exceeds a certain threshold chosen arbitrarily to 500 microns.

The same procedure is applied to the snow-graupel conversion due to riming, but in the present scheme snowflakes are defined as almost unrimed particles. Thus $\alpha_\circ$ is used as a tuning parameter to cause a rapid conversion by assuming $\alpha_{\circ,\text{snow}} = 0.01$.

The interactions by collisions of the various hydrometeors are summarized in Table 2 including secondary processes like riming-splintering and enhanced melting.

3.6 Melting of ice particles

An equation describing melting of ice particles is given by Pruppacher and Klett (1997) as

$$\frac{dx_i}{dt} = -\frac{2\pi}{L_{il}} D_g \left[K_T (T - T_3) F_h + \frac{D_v L_{iv}}{R_v}\left(\frac{p_v}{T} - \frac{p_{lv}(T_3)}{T_3}\right) F_v \right]. \tag{72}$$

In this equation, x_i and x_w are the masses of the ice and liquid water fraction, respectively, giving $x_i + x_w = \text{const.}$ (for the other variables see *List of symbols*). The ventilation coefficients for heat and water vapor are given by

$$F_v = a_{v,g} + b_{v,g} N_{Sc}^{1/3} N_{Re}^{1/2},$$
$$F_h = \frac{D_T}{D_v} F_v = \frac{K_T}{c_p \rho_0 D_v} F_v. \tag{73}$$

Thus, a characteristic time for melting is then (cf. Eq. (26))

$$\tau_{\text{melt}} = \frac{x_g}{\frac{dx_i}{dt}} = \frac{L_{il}}{2\pi}\frac{x_g}{D_g F_v}\left[\frac{K_T D_T}{D_v}(T - T_3) + \frac{D_v L_{iv}}{R_v}\left(\frac{p_v}{T} - \frac{p_{lv}(T_3)}{T_3}\right)\right]^{-1} \tag{74}$$

and results in equations for the time rates of change of the power moments reading

$$\begin{aligned}\frac{\partial M_g^n}{\partial t}\bigg|_{\text{melt}} &= -\int_0^\infty \frac{x^n f_g(x)}{\tau_{\text{melt}}}\, dx \\ &= -\frac{2\pi}{L_{il}}\left[\frac{K_T D_T}{D_v}(T - T_3) + \frac{D_v L_{iv}}{R_v}\left(\frac{p_v}{T} - \frac{p_{lv}(T_3)}{T_3}\right)\right] \\ &\quad \times \int_0^\infty D_g(x) F_v(x) f_g(x) x^{n-1} dx,\end{aligned} \tag{75}$$

and again we assume a generalized Γ-distribution for $f_g(x)$ and arrive at

$$\begin{aligned}\frac{\partial M_g^n}{\partial t}\bigg|_{\text{melt}} &= -\frac{2\pi}{L_{il}}\left[\frac{K_T D_T}{D_v}(T - T_3) + \frac{D_v L_{iv}}{R_v}\left(\frac{p_v}{T} - \frac{p_{lv}(T_3)}{T_3}\right)\right] \\ &\quad \times N_g\, D_g(\bar{x}_g) \bar{x}_g^{n-1}\, \bar{F}_{v,n}(\bar{x}_g)\end{aligned} \tag{76}$$

with the averaged ventilation coefficient given by

$$\bar{F}_{v,n}(\bar{x}) = \bar{a}_{\text{vent},n} + \bar{b}_{\text{vent},n} N_{Sc}^{1/3} N_{Re}^{1/2}(\bar{x}), \tag{77}$$

(see Appendix B). Equations (76)–(77) are applied to melting of all types of ice particles, namely graupel, snow and cloud ice. Evaporation from the liquid surface of melting particles is parameterized similar to evaporation of raindrops, but assuming a surface temperature of $T_3 = 273.16\,\text{K}$.

3.7 Sedimentation of ice particles

Sedimentation of cloud ice, snow and graupel is described using the same approach as for

raindrops and cloud droplets. Since the velocity–mass-relationships for cloud ice, snow and graupel are assumed as power laws and the size distributions are supposed to be generalized Γ-distributions, the mean fall velocities for the k-th moment of each particle type is given by

$$\bar{v}_{e,k}(\bar{x}) = \alpha_e \frac{\Gamma\left(\frac{k+\nu_e+\beta_e+1}{\mu_e}\right)}{\Gamma\left(\frac{k+\nu_e+1}{\mu_e}\right)} \left[\frac{\Gamma\left(\frac{\nu_e+1}{\mu_e}\right)}{\Gamma\left(\frac{\nu_e+2}{\mu_e}\right)}\right]^{\beta_e} \bar{x}_e^{\beta_e} \tag{78}$$

with $e \in \{i, s, g\}$.

4. Conclusions

We presented a parameterization of the most important cloud microphysical processes within mixed-phase clouds, especially mid-latitude deep convective clouds.

The proposed scheme is in some parts similar to parameterizations used in the well-established schemes of Lin et al (1983), Rutledge and Hobbs (1984), Murakami (1990) and Reisner et al (1998) to mention only some of the most important. On the other hand, some new approximations have been introduced: the warm phase part is an extension of the method described by Seifert and Beheng (2001) now taking into account turbulence effects, height dependent fall velocities, an improved selfcollection of raindrops as well as collisional breakup of raindrops. Nucleation of cloud droplets is parameterized directly as a function of the resolved supersaturation and the vertical velocity. The rate of change of number as well as mass densities by evaporation is described as a function of subsaturation and the sedimentation of droplets is treated by using two different weighted mean fall velocities. The ice phase processes are based on an improved Wisner-approximation for the collision integrals and size dependent mean collision efficiencies are included. Melting of ice particles and conversion to graupel due to riming are parameterized based on the characteristic time approach.

The physically based two-moment scheme presented in this paper intends to close the gap between the much simpler one-moment schemes and the expensive spectral bin models. The application of the two-moment approach to all types of cloud and precipitation particles enables the proposed scheme to simulate CCN effects on mixed-phase clouds. The scheme is still rather simple and computationally very efficient compared with the spectral bin models.

Further work has already been done on a comparison with the spectral bin method used within the Hebrew University Cloud Model (HUCM). The two-moment scheme presented here has shown a very good agreement with this highly sophisticated model (Seifert et al, 2005). A case study using this two-moment scheme within the atmospheric model KAMM2 to simulate a single isolated thunderstorm, which was observed in the Black Forest mountains, has also shown encouraging result (Bertram et al, 2004).

Improvements of the microphysical description of large graupel and hail particles, including wet growth and shedding, will be done in the future. Reliable in-situ and remote-sensing observations of microphysical variables are necessary to validate and improve the parameterization of the ice phase processes in general and especially of heterogenous nucleation. Implementations of the described scheme in the mesoscale limited-area models WRF and LM are available.

In Part 2, a sensitivity study is shown concerning the different evolution of idealized continental vs. maritime mixed-phase thunderstorms following the classical work of Weisman and Klemp (1982).

Appendix A

The generalized Γ-distribution

One of the most general analytical distribution function used to describe size distributions of hydrometeors is the so-called generalized Γ-distribution (hyper-gamma distribution or modified Γ-distribution; cf. Suzuki 1964, Flatau et al, 1989, Liu et al, 1995, Considine and Curry, 1996, Cohard and Pinty, 2000a, b; auf der Maur, 2001):

$$f(x) = A\, x^{\nu}\, \exp(-\lambda x^{\mu}) \tag{79}$$

(here with particle mass x). In case of $\mu = 1$ this function reduces to the classical Γ-distribution, with $\nu = \mu - 1$ to the Weibull distribution and with $\mu = 0$, $\nu = 0$ to the exponential distribution (as function of particle mass). The coefficients A

and λ can be expressed by the number and mass densities:

$$A = \frac{\mu N}{\Gamma\left(\frac{\nu+1}{\mu}\right)} \lambda^{\frac{\nu+1}{\mu}} \quad \text{and} \quad \lambda = \left[\frac{\Gamma\left(\frac{\nu+1}{\mu}\right)}{\Gamma\left(\frac{\nu+2}{\mu}\right)} \bar{x}\right]^{-\mu} \tag{80}$$

with the mean particle mass $\bar{x} = L/N$. According to these relations the generalized Γ-distribution can be easily written as a function of number and mass densities in the form:

$$f(x) = \frac{N}{\bar{x}} \left[\frac{x}{\bar{x}}\right]^{\nu} \frac{\mu}{\Gamma\left(\frac{\nu+1}{\mu}\right)} \left[\frac{\Gamma\left(\frac{\nu+2}{\mu}\right)}{\Gamma\left(\frac{\nu+1}{\mu}\right)}\right]^{\nu+1} \times \exp\left\{ -\left[\frac{\Gamma\left(\frac{\nu+2}{\mu}\right)}{\Gamma\left(\frac{\nu+1}{\mu}\right)} \frac{x}{\bar{x}}\right]^{\mu}\right\}. \tag{81}$$

The moments of power-n are then given by

$$M^n = \frac{\Gamma\left(\frac{n+\nu+1}{\mu}\right)}{\Gamma\left(\frac{\nu+1}{\mu}\right)} \left[\frac{\Gamma\left(\frac{\nu+1}{\mu}\right)}{\Gamma\left(\frac{\nu+2}{\mu}\right)}\right]^{n} N \bar{x}^n. \tag{82}$$

Note that an exponential distribution regarding to particle diameter D

$$f(D) = \hat{A} e^{-\hat{\lambda} D} \tag{83}$$

corresponds to

$$f(x) = A\, x^{-\frac{2}{3}} \exp(-\lambda x^{\frac{1}{3}}), \tag{84}$$

i.e., using x instead of D results directly in a generalized Γ-distribution. This shows that the so-called Marshall-Palmer distribution for raindrops is described by $\nu_r = -2/3$ and $\mu_r = 1/3$ (cf. Table 1).

Appendix B

Constants in weighted ventilation coefficients

In the parameterizations of evaporation, depositional growth and melting an averaged ventilation coefficient related to the n-th power moment occurs:

$$\bar{F}_{v,n}(\bar{x}) = \bar{a}_{\text{vent},n} + \bar{b}_{\text{vent},n} N_{Sc}^{1/3} N_{Re}^{1/2}(\bar{x}). \tag{85}$$

The constants $\bar{a}_{\text{vent},n}$ and $\bar{b}_{\text{vent},n}$ depend on the diameter–mass-relation $D(x) = a_a x^{b_a}$, the velocity–mass-relation $v(x) = \alpha_a x^{\beta_a}$ and the constant parameters ν_a and μ_a of the generalized gamma-distribution

$$f_a(x) = A x^{\nu_a} \exp(-\lambda x^{\mu_a}). \tag{86}$$

A straightforward calculation of

$$\int_0^{\infty} D(x) F_v(x) f(x) x^{n-1} dx = N\, D(\bar{x})\, \bar{x}^{n-1}\, \bar{F}_{v,n}(\bar{x}) \tag{87}$$

shows that two constants are given explicitly by

$$\bar{a}_{\text{vent},n} = a_v \frac{\Gamma\left(\frac{\nu_a+n+b_a}{\mu_a}\right)}{\Gamma\left(\frac{\nu_a+1}{\mu_a}\right)} \left[\frac{\Gamma\left(\frac{\nu_a+1}{\mu_a}\right)}{\Gamma\left(\frac{\nu_a+2}{\mu_a}\right)}\right]^{b_a+n-1}, \tag{88}$$

$$\bar{b}_{\text{vent},n} = b_v \frac{\Gamma\left(\frac{\nu_a+n+\frac{3}{2}b_a+\frac{1}{2}\beta_a}{\mu_a}\right)}{\Gamma\left(\frac{\nu_a+1}{\mu_a}\right)} \left[\frac{\Gamma\left(\frac{\nu_a+1}{\mu_a}\right)}{\Gamma\left(\frac{\nu_a+2}{\mu_a}\right)}\right]^{\frac{3}{2}b_a+\frac{1}{2}\beta_a+n-1}. \tag{89}$$

Appendix C

Constants in collision integrals

In the parameterizations of the different collision integrals various dimensionless constants appear, which depend on the diameter–mass- and velocity–mass-relations of the the particle types "a" and "b" and the constant parameters ν and μ of both particle ensembles. The details of this straightforward, but lengthy calculation can be found in Seifert (2002), for brevity the coefficients are given here without proof:

$$\delta_b^k = \frac{\Gamma\left(\frac{2b_b+\nu_b+1+k}{\mu_b}\right)}{\Gamma\left(\frac{\nu_b+1}{\mu_b}\right)} \left[\frac{\Gamma\left(\frac{\nu_b+1}{\mu_b}\right)}{\Gamma\left(\frac{\nu_b+2}{\mu_b}\right)}\right]^{2b_b+k}, \tag{90}$$

$$\delta_{ba}^k = 2\, \frac{\Gamma\left(\frac{b_a+\nu_a+1+k}{\mu_a}\right)}{\Gamma\left(\frac{\nu_a+1}{\mu_a}\right)} \frac{\Gamma\left(\frac{b_b+\nu_b+1}{\mu_b}\right)}{\Gamma\left(\frac{\nu_b+1}{\mu_b}\right)} \left[\frac{\Gamma\left(\frac{\nu_a+1}{\mu_a}\right)}{\Gamma\left(\frac{\nu_a+2}{\mu_a}\right)}\right]^{b_a+k} \times \left[\frac{\Gamma\left(\frac{\nu_b+1}{\mu_b}\right)}{\Gamma\left(\frac{\nu_b+2}{\mu_b}\right)}\right]^{b_b}, \tag{91}$$

$$\vartheta_b^k = \frac{\Gamma\left(\frac{2\beta_b+2b_b+\nu_b+1+k}{\mu_b}\right)}{\Gamma\left(\frac{2b_b+\nu_b+1+k}{\mu_b}\right)} \left[\frac{\Gamma\left(\frac{\nu_b+1}{\mu_b}\right)}{\Gamma\left(\frac{\nu_b+2}{\mu_b}\right)}\right]^{2\beta_b}, \tag{92}$$

$$\vartheta_{ba}^k = 2\, \frac{\Gamma\left(\frac{\beta_a+b_a+\nu_a+1+k}{\mu_a}\right)}{\Gamma\left(\frac{b_a+\nu_a+1+k}{\mu_a}\right)} \frac{\Gamma\left(\frac{\beta_b+b_b+\nu_b+1}{\mu_b}\right)}{\Gamma\left(\frac{b_b+\nu_b+1}{\mu_b}\right)} \times \left[\frac{\Gamma\left(\frac{\nu_a+1}{\mu_a}\right)}{\Gamma\left(\frac{\nu_a+2}{\mu_a}\right)}\right]^{\beta_a} \left[\frac{\Gamma\left(\frac{\nu_b+1}{\mu_b}\right)}{\Gamma\left(\frac{\nu_b+2}{\mu_b}\right)}\right]^{\beta_b}. \tag{93}$$

Please note $\delta_{ba}^1 \neq \delta_{ab}^1$ and $\vartheta_{ba}^1 \neq \vartheta_{ab}^1$, since "$a$" is collecting "$b$" there is obviously no symmetry with respect to "a" and "b".

Appendix D

Limiting raindrop size distributions

To avoid artificial sedimentation or evaporation due to unrealistic size distributions or mean masses, especially for $N \to 0$ and $L \to 0$ when $\bar{x}_r = L_r/N_r$ is not well defined, the following limiting procedure is applied:

$$\tilde{x}_r = \max\left(\bar{x}_{r,\min}, \min\left(\bar{x}_{r,\min}, \frac{L_r}{N_r}\right)\right), \tag{94}$$

$$N_0 = \max\left(N_{0,\min}, \min\left(N_{0,\max}, N_r\left(\frac{\pi\rho_w}{\tilde{x}_r}\right)^{\frac{1}{3}}\right)\right), \tag{95}$$

$$\lambda_r = \max\left(\lambda_{\min}, \min\left(\lambda_{\max}, \left(\frac{\pi\rho_w N_0}{L_r}\right)^{\frac{1}{4}}\right)\right), \tag{96}$$

$$\bar{x}_r = \max\left(\bar{x}_{r,\min}, \min\left(\bar{x}_{r,\min}, \frac{L_r\lambda_r}{N_0}\right)\right) \tag{97}$$

with $N_{0,\min} = 2.5\times10^5\,\mathrm{m}^{-4}$, $N_{0,\max} = 2\times10^7\,\mathrm{m}^{-4}$, $\lambda_{\min} = 1\times10^3\,\mathrm{m}^{-1}$ and $\lambda_{\max} = 1\times10^4\,\mathrm{m}^{-1}$. In case of sedimentation λ_r as given by Eq. (96) is used to calculated the mean fall velocities by Eq. (21), while for evaporation $\bar{x}_r$ as given by Eq. (97) is used instead of the simple $\bar{x}_r = L_r/N_r$ or Eq. (94). Note that Eqs. (94)–(97) are only correct for $\nu_r = -2/3$ and $\mu_r = 1/3$.

List of symbols

Notation	Description	Value	Unit
α	constant in fallspeed relation		$\mathrm{m\,s^{-1}\,kg^{-\beta}}$
α_c	constant in fallspeed relation for cloud droplets	3.75×10^5	$\mathrm{m\,s^{-1}\,kg^{-\beta_c}}$
α_r	constant in fallspeed relation for raindrops	159.0	$\mathrm{m\,s^{-1}\,kg^{-\beta_r}}$
α_g	constant in fallspeed relation for graupel	46.40	$\mathrm{m\,s^{-1}\,kg^{-\beta_g}}$
α_i	constant in fallspeed relation for cloud ice	317.0	$\mathrm{m\,s^{-1}\,kg^{-\beta_i}}$
α_s	constant in fallspeed relation for snowflakes	27.70	$\mathrm{m\,s^{-1}\,kg^{-\beta_s}}$
$\alpha_\circ$	space filling constant	0.68	
$\alpha_{\circ,\mathrm{snow}}$	space filling constant for snow	0.01	
β	constant in fallspeed relation		
β_c	constant in fallspeed relation for cloud droplets	2/3	
β_r	constant in fallspeed relation for raindrops	0.266	
β_g	constant in fallspeed relation for graupel	0.260	
β_i	constant in fallspeed relation for cloud ice	0.362	
β_s	constant in fallspeed relation for snowflakes	0.220	
δ_a^k	constant in improved Wisner-approximation		
δ_{ab}^k	constant in improved Wisner-approximation		
Δt	time step		s
$\overline{\Delta v_{ab}}$	mean difference of fallspeeds		$\mathrm{m\,s^{-1}}$
ϑ_a^k	constant in improved Wisner-approximation		
ϑ_{ab}^k	constant in improved Wisner-approximation		
ε	turbulent dissipation		$\mathrm{m^2\,s^{-3}}$
$\Gamma(x)$	gamma function		
λ	slope in size distribution		$\mathrm{kg^{-\mu}}$
λ_r	slope in raindrop size distribution		$\mathrm{kg^{-\mu_r}}$
μ	constant in generalized Γ-distribution		
μ_c	constant in generalized Γ-distribution for cloud droplets		
μ_r	constant in generalized Γ-distribution for raindrops		
μ_g	constant in generalized Γ-distribution for graupel		
μ_i	constant in generalized Γ-distribution for cloud ice		
μ_s	constant in generalized Γ-distribution for snowflakes		
ν	constant in generalized Γ-distribution		
ν_c	constant in generalized Γ-distribution for cloud droplets		
ν_r	constant in generalized Γ-distribution for raindrops		
ν_g	constant in generalized Γ-distribution for graupel		
ν_i	constant in generalized Γ-distribution for cloud ice		
ν_s	constant in generalized Γ-distribution for snowflakes		

(*continued*)

List of symbols (*continued*)

ν_{air}	kinematic viscosity of air	1.4086×10^{-5}	$\text{m}^2\,\text{s}^{-1}$
κ	constant in CCN relation		
κ_{rr}	constant in approximate collision kernel	60.7	$\text{kg}^{-1/3}$
ρ_0	air density at surface conditions	1.225	$\text{kg}\,\text{m}^{-3}$
ρ	air density		$\text{kg}\,\text{m}^{-3}$
ρ_w	density of water	1000	$\text{kg}\,\text{m}^{-3}$
ρ_ε	density of ice	900	$\text{kg}\,\text{m}^{-3}$
σ_i	variance of fallspeed for cloud ice	0.2	$\text{m}\,\text{s}^{-1}$
σ_s	variance of fallspeed for snowflakes	0.2	$\text{m}\,\text{s}^{-1}$
τ	characteristic time of coagulation		
τ_{conv}	characteristic time of conversion		s
τ_{eva}	characteristic time of evaporation		s
Φ_{au}	universal function for autoconversion		
Φ_{au}	universal function for accretion		
Φ_{br}	universal function for breakup		
a	constant in diameter-mass-relation		$\text{m}\,\text{kg}^{-b}$
a_c	constant in diameter-mass-relation for cloud droplets	0.124	$\text{m}\,\text{kg}^{-b_c}$
a_r	constant in diameter-mass-relation for raindrops	0.124	$\text{m}\,\text{kg}^{-b_r}$
a_g	constant in diameter-mass-relation for graupel	0.190	$\text{m}\,\text{kg}^{-b_g}$
a_i	constant in diameter-mass-relation for cloud ice	0.217	$\text{m}\,\text{kg}^{-b_i}$
a_s	constant in diameter-mass-relation for snowflakes	8.156	$\text{m}\,\text{kg}^{-b_s}$
a_v	constant in ventilation coefficient		
$a_{v,r}$	constant in ventilation coefficient for raindrops	0.78	
$a_{v,g}$	constant in ventilation coefficient for graupel	0.78	
$a_{v,i}$	constant in ventilation coefficient for cloud ice	0.86	
$a_{v,s}$	constant in ventilation coefficient for snowflakes	0.78	
$\bar{a}_{\text{vent},n}$	constant in n-th mean ventilation coefficient		
a_{M92}	constant in Meyers formula	-0.639	
A_{het}	constant in Bigg's freezing formula	0.2	$\text{kg}^{-1}\,\text{s}^{-1}$
b	constant in diameter-mass-relation		
b_c	constant in diameter-mass-relation for cloud droplets		
b_r	constant in diameter-mass-relation for raindrops		
b_g	constant in diameter-mass-relation for graupel		
b_i	constant in diameter-mass-relation for cloud ice		
b_s	constant in diameter-mass-relation for snow		
b_v	constant in ventilation coefficient		
$b_{v,r}$	constant in ventilation coefficient for raindrops	0.308	
$b_{v,g}$	constant in ventilation coefficient for graupel	0.308	
$b_{v,i}$	constant in ventilation coefficient for cloud ice	0.280	
$b_{v,s}$	constant in ventilation coefficient for snowflakes	0.308	
$\bar{b}_{\text{vent},n}$	constant in n-th mean ventilation coefficient		
b_{M92}	constant in Meyers formula	12.96	
B_{het}	constant in Bigg's freezing formula	0.65	K^{-1}
c_c	constant in capacity for cloud droplets	2	
c_r	constant in capacity for raindrops	2	
c_g	constant in capacity for graupel	2	
c_i	constant in capacity for cloud ice	π	
c_s	constant in capacity for snow	2	
c_w	specific heat of water	4.187×10^6	$\text{J}\,\text{kg}^{-1}\,\text{K}^{-1}$
C_{ccn}	constant in CCN relation		m^{-3}
D	(maximum) diameter of particles		m
D_c	diameter of cloud droplets		m
D_r	diameter of raindrops		m
D_g	diameter of graupel		m
D_i	diameter of cloud ice		m
D_s	diameter of snowflakes		m
$\bar{D}$	mean (maximum) diameter		m
$\bar{D}_c$	mean diameter of cloud droplets		m

(*continued*)

List of symbols (*continued*)

$\bar{D}_r$	mean diameter of raindrops		m
$\bar{D}_g$	mean diameter of graupel		m
$\bar{D}_i$	mean diameter of cloud ice		m
$\bar{D}_s$	mean diameter of snowflakes		m
$\bar{D}_{c,0}$	constant in collision efficiency for cloud droplets	15×10^{-6}	m
$\bar{D}_{c,1}$	constant in collision efficiency for cloud droplets	40×10^{-6}	m
$\bar{D}_{g,0}$	constant in collision efficiency for graupel	150×10^{-6}	m
$\bar{D}_{i,0}$	constant in collision efficiency for cloud ice	150×10^{-6}	m
$\bar{D}_{s,0}$	constant in collision efficiency for snowflakes	150×10^{-6}	m
$\bar{D}_{eq}$	equlibrium diameter	0.9×10^{-3}	m
D_v	diffusivity of water vapor	3.0×10^{-5}	$\mathrm{m^2\,s^{-1}}$
D_T	diffusivity of heat		$\mathrm{m^2\,s^{-1}}$
E_{stick}	sticking efficiency		1
$\bar{E}_{g,\max}$	maximum mean collision efficiency for graupel	1.0	1
$\bar{E}_{i,\max}$	maximum mean collision efficiency for cloud ice	0.8	1
$\bar{E}_{s,\max}$	maximum mean collision efficiency for snowflakes	0.8	1
f	number density size distribution		$\mathrm{m^{-3}\,kg^{-1}}$
f_w	number density size distribution for droplets		$\mathrm{m^{-3}\,kg^{-1}}$
f_c	number density size distribution for cloud droplets		$\mathrm{m^{-3}\,kg^{-1}}$
f_r	number density size distribution for raindrops		$\mathrm{m^{-3}\,kg^{-1}}$
f_g	number density size distribution for graupel		$\mathrm{m^{-3}\,kg^{-1}}$
f_i	number density size distribution for cloud ice		$\mathrm{m^{-3}\,kg^{-1}}$
F_h	ventilation coefficient for heat		1
F_v	ventilation coefficient for water vapor		1
$\bar{F}_{v,n}$	mean ventilation coefficient for the n-th moment		1
F_{splint}	production rate of splinters per rime mass		$\mathrm{kg^{-1}}$
J_{het}	temperature function for heterogenous freezing		$\mathrm{kg^{-1}\,s^{-1}}$
J_{hom}	temperature function for homogenous freezing		$\mathrm{kg^{-1}\,s^{-1}}$
k_{br}	constant in breakup parameterization	1.0×10^3	$\mathrm{m^{-1}}$
k_{cc}	constant in cloud–cloud kernel	4.44×10^9	$\mathrm{m^3\,kg^{-2}\,s^{-1}}$
k'_{cc}	constant in turbulent cloud droplet kernel	10.58×10^9	$\mathrm{m^3\,kg^{-2}\,s^{-1}}$
k_{cr}	constant in cloud–rain kernel	5.25	$\mathrm{m^3\,kg^{-1}\,s^{-1}}$
k_{rr}	constant in rain–rain kernel	7.12	$\mathrm{m^3\,kg^{-1}\,s^{-1}}$
K_{ab}	collection kernel		$\mathrm{m^3\,s^{-1}}$
K_h	turbulent diffusivity for heat		$\mathrm{m^2\,s^{-1}}$
K_T	conductivity of heat	2.5×10^{-2}	$\mathrm{J\,m^1\,s^{-1}\,K^{-1}}$
L_w	mass density of droplets/liquid water content		$\mathrm{kg\,m^{-3}}$
L_c	mass density of cloud droplets/cloud water content		$\mathrm{kg\,m^{-3}}$
L_r	mass density of raindrops/rain water content		$\mathrm{kg\,m^{-3}}$
L_g	mass density of graupel		$\mathrm{m^{-3}}$
L_i	mass density of cloud ice		$\mathrm{m^{-3}}$
L_s	mass density of snowflakes		$\mathrm{m^{-3}}$
L_{lv}	latent heat of evaporation	2.501×10^6	$\mathrm{J\,kg^{-1}}$
L_{iv}	latent heat of sublimation	2.834×10^6	$\mathrm{J\,kg^{-1}}$
L_{il}	latent heat of melting	0.333×10^6	$\mathrm{J\,kg^{-1}}$
M_w^k	k-th power moment of $f_w(x)$		$\mathrm{kg^k\,m^{-3}}$
M_c^k	k-th power moment of $f_c(x)$ (cloud droplets)		$\mathrm{kg^k\,m^{-3}}$
M_r^k	k-th power moment of $f_r(x)$ (raindrops)		$\mathrm{kg^k\,m^{-3}}$
N_c	number density of cloud droplets		$\mathrm{m^{-3}}$
N_r	number density of raindrops		$\mathrm{m^{-3}}$
N_g	number density of graupel		$\mathrm{m^{-3}}$
N_i	number density of cloud ice		$\mathrm{m^{-3}}$
N_s	number density of snowflakes		$\mathrm{m^{-3}}$
N_w	number density of droplets		$\mathrm{m^{-3}}$
N_{ccn}	number density of cloud condensation nuclei		$\mathrm{m^{-3}}$
N_{Re}	Reynolds number		1
N_{Sc}	Schmidt number	0.71	1
N_{M92}	constant in Meyers formula	1×10^3	$\mathrm{m^{-3}}$

(*continued*)

List of symbols (*continued*)

$\mathcal{N}$	normalization factor		$\mathrm{kg\,m^{-4}}$
p	pressure		Pa
p_{lv}	saturation vapor pressure over liquid water		Pa
p_{iv}	saturation vapor pressure over ice		Pa
P	velocity distribution		$\mathrm{s\,m^{-1}}$
r_*	separating drop radius	40×10^{-6}	$\mathrm{m^{-1}}$
R_m	specific gas constant for moist air		$\mathrm{J\,kg^{-1}\,K^{-1}}$
R_v	specific gas constant for water vapor	461.51	$\mathrm{J\,kg^{-1}\,K^{-1}}$
R_a	specific gas constant for dry air	287.05	$\mathrm{J\,kg^{-1}\,K^{-1}}$
S	supersaturation over water		
S_i	supersaturation over ice		
T	temperature		K
T_c	Celsius temperature		°C
T_3	temperature of freezing point	273.15	K
t	time		s
$\vec{v}$	wind velocity		$\mathrm{m\,s^{-1}}$
v_c	terminal fall velocity of cloud droplets		$\mathrm{m\,s^{-1}}$
v_r	terminal fall velocity of raindrops		$\mathrm{m\,s^{-1}}$
v_g	terminal fall velocity of graupel		$\mathrm{m\,s^{-1}}$
v_i	terminal fall velocity of cloud ice		$\mathrm{m\,s^{-1}}$
v_s	terminal fall velocity of snowflakes		$\mathrm{m\,s^{-1}}$
$\bar{v}_{a,k}$	mean fallspeed of k-th moment of particle 'a'		$\mathrm{m\,s^{-1}}$
w	vertical wind velocity		$\mathrm{m\,s^{-1}}$
x	mass of particles		kg
x^*	separating drop mass	2.6×10^{-10}	kg
$\bar{x}_c$	mean mass of cloud droplets		kg
$\bar{x}_r$	mean mass of raindrops		kg
$\bar{x}_g$	mean mass of graupel		kg
$\bar{x}_i$	mean mass of cloud ice		kg
$\bar{x}_s$	mean mass of snowflakes		kg
$x_{c,nuc}$	mass of nucleated cloud droplets	1.0×10^{-12}	kg
y	mass of particles		kg
z	vertical length coordinate		m
Z	second moment of size distribution $f(x)$		$\mathrm{kg^2\,m^{-3}}$

Acknowledgments

We gratefully acknowledge fruitful discussions with Prof. A. Khain, Dr. M. Pinsky and Dr. U. Wacker. Parts of this work (A. Seifert) have been funded by BMBF grant no. 02WT0249 (German – Israeli cooperation in water technology).

References

auf der Maur AN (2001) Statistical tools for drop size distributions: Moments and generalized gamma. J Atmos Sci 58: 407–418

Beard KV, Ochs HT (1995) Collisions between small precipitation drops. Part II: Formulas for coalescence, temporary coalescence, and satellites. J Atmos Sci 52: 3977–3996

Beheng KD (1981) Stochastic riming of plate-like and columnar ice crystals. Pure Appl Geophys 119: 820–830

Beheng KD (1982) A numerical study on the combined action of droplet coagulation, ice particle riming and the splintering process concerning maritime cumuli. Contrib Atmos Phys 55: 201–214

Beheng KD (1994) A parameterization of warm cloud microphysical conversion processes. Atmos Res 33: 193–206

Beheng KD, Doms G (1986) A general formulation of collection rates of cloud and raindrops using the kinetic equation and comparison with parameterizations. Contrib Atmos Phys 59: 66–84

Berry EX (1968) Modification of the warm rain process. In: Proc. 1st Natl. Conf. Wea. Modification, Boston, pp 81–85. Amer Meteor Soc

Bertram I, Seifert A, Beheng KD (2004) The evolution of liquid/ice content of a mid-latitude convective storm derived from radar data and results from a cloud-resolving model. Meteorol Zeitschr 13: 221–232

Bigg EK (1953) The formation of atmospheric ice crystals by the freezing of droplets. Quart J Roy Meteor Soc 79: 510–519

Cohard J-M, Pinty J-P (2000a) A comprehensive two-moment warm microphysical bulk scheme. I: Description and tests. Quart J Roy Meteor Soc 126: 1815–1842

Cohard J-M, Pinty J-P (2000b) A comprehensive two-moment warm microphysical bulk scheme. II: 2D

experiments with a non-hydrostatic model. Quart J Roy Meteor Soc 126: 1843–1859

Cohard J-M, Pinty J-P, Bedos C (1998) Extending Twomey's analytical estimate of nucleated cloud droplet concentrations from CCN spectra. J Atmos Sci 55: 3348–3357

Cohard J-M, Pinty J-P, Suhre K (2000) On the parameterization of activation spectra from cloud condensation nuclei microphysical properties. J Geophys Res 105: 11753–11766

Considine G, Curry JA (1996) A statistical model of drop-size spectra for stratocumulus clouds. Quart J Roy Meteor Soc 122: 611–634

Cotton R, Field P (2002) Ice nucleation characteristics of an isolated wave cloud. Quart J Roy Meteor Soc 128: 2417–2437

Cotton W, Pielke R, Walko R, Liston G, Tremback C, Jiang H, McAnelly R, Harrington J, Nicholls M, Carrio C, McFadden J (2003) RAMS 2001: Current status and future directions. Meteorol Atmos Phys 82: 5–29

Cotton WR, Stephens MA, Nehrkorn T, Tripoli GJ (1982) The Colorado State University three-dimensional cloud/mesoscale model – 1982. Part II: An ice-phase parameterization. J Rech Atmos 16: 295–320

Cotton WR, Tripoli GJ, Rauber RM, Mulvihill EA (1986) Numerical simulation of the effects of varying ice crystal nucleation rates and aggregation processes on orographic snowfall. J Clim Appl Meteor 25: 1658–1680

Doms G, Beheng KD (1986) Mathematical formulation of self-collection, autoconversion and accretion rates of cloud and raindrops. Meteorol Rdsch 39: 98–102

Feingold G, Walko RL, Stevens B, Cotton WR (1998) Simulations of marine stratocumulus using a new microphysical parameterization scheme. Atmos Res 47–48: 505–528

Ferrier BS (1994) A double-moment multiple-phase four-class bulk ice scheme. Part I: Description. J Atmos Sci 51: 249–280

Flatau PJ, Tripoli GJ, Verlinde J, Cotton WR (1989) The CSU-RAMS Cloud Microphysics Module: General Theory and Code Documentation. Department of Atmospheric Sciences, Colorado State University

Hall WD, Pruppacher HR (1976) The survival of ice particles falling from cirrus clouds in subsaturated air. J Atmos Sci 33: 1995–2006

Harrington JY, Meyers MP, Walko RL, Cotton WR (1995) Parameterization of ice crystal conversion processes due to vapor deposition for mesoscale models using double-moment basis functions. Part I: Basic formulation and parcel model results. J Atmos Sci 52: 4344–4366

Heymsfield AJ, Kajikawa M (1987) An improved approach to calculating terminal velocities of plate-like crystals and graupel. J Atmos Sci 44: 1088–1099

Hu Z, Srivastava RC (1995) Evolution of raindrop size distribution by coalescence, breakup, and evaporation: Theory and observations. J Atmos Sci 52: 1761–1783

Jeffrey CA, Austin PH (1997) Homogenous nucleation of supercooled water: Results from a new equation of state. J Geophys Res 102: 25269–25279

Kessler E (1969) On the distribution and continuity of water substance in atmospheric circulations. Meteor Monogr 32. Boston: Amer Meteor Soc

Khain A, Ovtchinnikov M, Pinsky M, Pokrovsky A, Krugliak H (2000) Notes on the state-of-the-art numerical modeling of cloud microphysics. Atmos Res 55: 159–224

Khain AP, Rosenfeld D, Pokrovsky A (2001) Simulating convective clouds with sustained supercooled liquid water down to −37.5 °C using a spectral microphysics model. Geophys Res Lett 28: 3887–3890

Kogan YL, Martin WJ (1994) Parameterization of bulk condensation in numerical cloud models. J Atmos Sci 51: 1728–1739

Lin Y-L, Farley RD, Orville H (1983) Bulk parameterization of the snow field in a cloud model. J Clim Appl Meteorol 22: 1065–1092

List R (1988) A linear radar reflectivity-rainrate relationship for steady tropical rain. J Atmos Sci 45: 3564–3572

Liu Y, Laiguang Y, Weinong Y, Feng L (1995) On the size distribution of cloud droplets. Atmos Res 35: 201–216

Locatelli JD, Hobbs PV (1974) Fall speeds and masses of solid precipitation particles. J Geophys Res 79: 2185–2197

Long AB (1974) Solutions to the droplet collection equation for polynomial kernels. J Atmos Sci 31: 1040–1052

Low TB, List R (1982) Collision, coalescence and breakup of raindrops. Part I: Experimentally established coalescence efficiencies and fragment size distributions in breakup. J Atmos Sci 39: 1591–1606

Manton M, Cotton W (1977) Formulation of approximate equations for modeling moist convection on the mesoscale. Technical report, Colorado State University

Mayer F (2000) Numerische Simulation des Zerfallsprozesses von Regentropfen. Diploma thesis, Institut für Meteorologie und Klimaforschung, Universität Karlsruhe/Forschungszentrum Karlsruhe, Karlsruhe (in German)

Meyers MP, DeMott PJ, Cotton WR (1992) New primary ice-nucleation parameterizations in an explicit cloud model. J Appl Meteor 31: 708–721

Meyers MP, Walko RL, Harrington JY, Cotton WR (1997) New RAMS cloud microphysics parameterization. Part II: The two-moment scheme. Atmos Res 45: 3–39

Mizuno H (1990) Parameterization of the accretion process between different precipitation elements. J Meteor Soc Jap 68: 395–398

Murakami M (1990) Numerical modeling of dynamical and microphysical evolution of an isolated convective cloud – The 19 July 1981 CCOPE cloud. J Meteor Soc Jap 68: 107–128

Pinsky M, Khain A (2002) Effects of in-cloud nucleation and turbulence on droplet spectrum formation in cumulus clouds. Quart J Roy Meteor Soc 128: 501–533

Pinsky M, Khain A, Shapiro M (2000) Stochastic effects of cloud droplet hydrodynamic interaction in a turbulent flow. Atmos Res 53: 131–169

Pinsky M, Khain A, Shapiro M (2001) Collision efficiency of drops in a wide range of Reynolds numbers: Effect of pressure on spectrum evolution. J Atmos Sci 58: 742–764

Pruppacher HR, Klett JD (1997) Microphysics of clouds and precipitation. Dordrecht: Kluwer Academic Publishers

Reisner J, Rasmussen RM, Bruintjes RT (1998) Explicit forecasting of supercooled liquid water in winter storms using the MM5 mesoscale model. Quart J Roy Meteor Soc 124: 1071–1107

Rogers RR, Baumgardner D, Ethier SA, Carter DA, Ecklund WL (1993) Comparison of raindrop size distributions measured by radar wind profiler and by airplane. J Appl Meteor 32: 694–699

Rosenfeld D (2000) Suppression of rain and snow by urban and industrial air pollution. Science 287: 1793–1796

Rutledge SA, Hobbs PV (1984) The mesoscale and microscale structure and organization of clouds and precipitation in mid latitude cyclones XII: A diagnostic modeling study of precipitation development in narrow cold-frontal rainbands. J Atmos Sci 41: 2949–2972

Seifert A (2002) Parametrisierung wolkenmikrophysikalischer Prozesse und Simulation konvektiver Mischwolken. Ph. D. thesis, Institut für Meteorologie und Klimaforschung, Universität Karlsruhe/Forschungszentrum Karlsruhe, Karlsruhe (in German)

Seifert A, Beheng KD (2001) A double-moment parameterization for simulating autoconversion, accretion and self-collection. Atmos Res 59–60: 265–281

Seifert A, Khain A, Pokrovsky A, Beheng KD (2005) A comparison of spectral bin and two-moment bulk mixed phase cloud microphysics. Atmos Res (in print)

Suzuki E (1964) Hyper gamma distribution and its fitting to rainfall data. Pap Meteor Geophys 15: 31–51

Tao W-K, Simpson J, Baker D, Braun S, Chou M-D, Ferrier B, Johnson D, Khain A, Lang S, Lynn B, Shie C-L, Starr D, Sui C-H, Wang Y, Wetzel P (2003) Microphysics, radiation and surface processes in the Goddard Cumulus Ensemble (GCE) model. Meteorol Atmos Phys 82: 97–137

Verlinde J, Cotton WR (1993) Fitting microphysical observations of nonsteady convective clouds to a numerical model: An application of the adjoint technique of data assimilation to a kinematic model. Mon Wea Rev 121: 2776–2793

Vohl O, Mitra SK, Wurzler SC, Pruppacher HR (1999) A wind tunnel study of the effects of turbulence on the growth of cloud drops by collision and coalescence. J Atmos Sci 56: 4088–4099

Wacker U, Seifert A (2001) Evolution of rain water profiles resulting from pure sedimentation: Spectral vs. parameterized description. Atmos Res 58: 19–39

Weisman ML, Klemp JB (1982) The dependency of numerically simulated convective storms on vertical wind shear and bouyancy. Mon Wea Rev 110: 504–520

Wisner C, Orville HD, Myers C (1972) A numerical model of a hail-bearing cloud. J Atmos Sci 29: 1160–1181

Zawadzki I, de Agostinho AM (1988) Equilibrium raindrop size distributions in tropical rain. J Atmos Sci 45: 3452–3459

Ziegler CL (1985) Retrieval of thermal and microphysical variables in observed convective storms. Part I: Model development and preliminary testing. J Atmos Sci 42: 1487–1509

Corresponding author's address: Axel Seifert, Deutscher Wetterdienst, GB Forschung und Entwicklung, Kaiserleistr. 42, 63067 Offenbach, Germany (E-mail: axel.seifert@dwd.de)